Revista Brasileira de Entomologia 63 (2019) 183–194

SOCIEDADE BRASILEIRA DE ENTOMOLOGIA FUNDADA EM 1937

REVISTA BRASILEIRA DE
Entomologia
A Journal on Insect Diversity and Evolution

www.rbentomologia.com

Systematics, Morphology and Biogeography

A redescription of *Antispastis clarkei* Pastrana (Lepidoptera, Glyphipterigidae) immature stages, with notes on the life history and phylogenetic placement of the genus

Gilson R.P. Moreira [a,*], Rosângela Brito [a], Rosy M.S. Isaias [b], JorgeL. Silveira Jr [a], Gislene L. Gonçalves [c,d]

[a] *Universidade Federal do Rio Grande do Sul, Instituto de Biociências, Departamento de Zoologia, Porto Alegre, RS, Brazil*
[b] *Universidade Federal de Minas Gerais, Instituto de Ciências Biológicas, Departamento de Botânica, Belo Horizonte, MG, Brazil*
[c] *Universidade Federal do Rio Grande do Sul, Instituto de Biociências, Departamento de Genética, Porto Alegre, RS, Brazil*
[d] *Universidad de Tarapacá, Facultad de Ciencias Agronómicas, Departamento de Recursos Ambientales, Arica, Chile*

ARTICLE INFO

Article history:
Received 7 December 2018
Accepted 7 March 2019
Available online 21 March 2019
Associate Editor: Héctor Vargas

Keywords:
Leaf-mining moths
Glyphipterigids
Acrolepiinae
Neotropical region
Natural history

ABSTRACT

Antispastis Meyrick, 1926 is a poorly known genus of leaf-mining micromoths endemic to the Neotropics, with still uncertain taxonomic position within the Yponomeutoidea. In the present study, the egg, larva and pupa of *A. clarkei* Pastrana, previously known only from Argentina, are described and illustrated with the aid of optical and scanning electron microscopy. Data on life history, including histology of the mine, are also provided. Family placement of the genus is reassessed based on comparison of morphology and DNA sequences with closely related lineages. The larvae form blotch mines on the upper surface of *Solanum* L. (Solanaceae) leaves, feeding on palisade parenchyma in all instars. Pupation occurs outside the mine, in an inverted basket-like, large-meshed cocoon constructed on the plant surface. DNA analysis of Cytochrome oxidase I gene of *A. clarkei* revealed interspecific differences averaging 10% with *A. xylophragma*, which provided species separation matching morphological differences. *Antispastis* was closely related phylogenetically to *Digitivalva*, clustering in the Acrolepiinae together with the genera *Acrolepia* and *Acrolepiopsis*, and ultimately placed within Glyphipterigidae. The geographical distribution of *A. clarkei* is expanded to the Southern Atlantic forest (Rio Grande do Sul and Paraná states, Brazil).

Introduction

Antispastis was proposed by Meyrick (1926) to include *A. xylophragma* Meyrick, 1926 which was described from a single male from Peru. It is a small, poorly known genus of micromoths restricted in distribution to the Neotropical region, including two additional species: *A. clarkei* Pastrana, 1951 from Argentina and *A. selectella* (Walker, 1863), from Brazil. Its taxonomy has been based on adult morphology, particularly on the mouthparts, wing venation and genitalia. These characters were illustrated by Clarke (1969) for *A. xylophragma*. Those of *A. clarkei* were presented in the original description (Pastrana, 1951), and for *A. selectella* by Davis (1980), who moved the latter species from *Adela* Latreille (Adelidae) to *Antispastis*. *A. selectella* had been originally described by Walker (1863) within *Micropteryx* Hübner (Micropterigidae), and later transferred to *Adela* by Meyrick (1912).

The taxonomic history of *Antispastis* has been confused at the family level. The genus was originally placed by Meyrick (1926) within the Glyphipterigidae (Yponomeutoidea). Davis (1980) moved it to Acrolepiidae based on morphological characters of the adults. This placement was later supported by Heppner (1987, 1984), based on larval morphology. However, this taxonomic placement has not been a consensus. For example, Gaedike (1997) considered Acrolepiidae with including three genera: *Acrolepia* Curtis, *Acrolepsiopsis* Gaedike and *Digitivalva* Gaedike, thus not including *Antispastis*. The status of Acrolepiidae has been also under debate. It has been considered by either as a family (Gaedike, 1997), or a subfamily (Acrolepiinae) either of Plutellidae (*e.g.* Kyrby 1984) or Glyphipterigidae (*e.g.* Nieukerken et al., 2011, Sohn et al., 2013), the classification followed here. These two families are sister taxa (Mutanen et al., 2010). The morphology of the immature stages is poorly known for Yponomeutoidea lineages in general, particularly regarding *Antispastis*, which makes further assessment of its taxonomic placement difficult.

In recent surveys on leaf-mining moths by the senior author in southernmost Brazil, leaf mines constructed by *Antispastis* larvae

* Corresponding author.
E-mail: gilson.moreira@ufrgs.br (G.R. Moreira).

https://doi.org/10.1016/j.rbe.2019.03.001

were collected from a few *Solanum* L. (Solanaceae) species. Adults reared in the laboratory conform to *A. clarkei*, previously known only from Buenos Aires, Argentina; its larva, pupa and the mine were described and illustrated under light microscopy by Bourquin (1951). In this study we provide a detailed description of the integument morphology of the egg, larva, and pupa with scanning electron microscopy. Notes are added on the life history from a population associated with *Solanum johannae* Bitter from the Atlantic Forest in the Rio Grande do Sul state, Brazil, including the histology of the leaf mine. We also present a phylogenetic inference based on DNA barcode sequences of *Antispastis*, including putative members of related genera of Acrolepiinae.

Materials and methods

Molecular analysis

Genomic DNA was extracted from three specimens of *A. clarkei* (LMCI 283-38A, B and C) using PureLink® Genomic DNA kit (Thermo Fisher Scientific, California, USA) according to the manufacturer's protocol. A fragment of 660 base pairs of the cytochrome oxidase subunit I (COI) was amplified via PCR using primers LCO1490 and HCO2198 and standard conditions (Folmer et al., 1994). PCR products were purified with exonuclease and alkaline phosphatase (Fermentas, Vilnius, Lithuania) and sequenced using an ABI 3730 (Thermo Fisher Scientific) capillary sequencer. Sequences were aligned and variable sites checked using CodonCode Aligner 3.7.1. (CodonCode Corporation, Centerville, USA). DNA sequences are deposited in GenBank (MK279396, MK279397, MK279398) and available in BOLD (Barcode of Life Data Systems; www.barcodinglife.org) (Ratnasingham and Hebert, 2007) through the public dataset: DS-NEOANTI (Table 1).

To infer the phylogenetic position of *A. clarkei*, we first blasted the LMCI 238-38A sequence in BOLD: it was closer to Acrolepiinae (similarity of 88% to other genera), in agreement with morphology-based inferences. Then we downloaded all sequences available from this subfamily to conduct the phylogenetic analysis. We kept one specimen per species and removed those that clearly represented misidentification (e.g. *Antispastis* sp., BOLD sequence LNOUF263-11.COI-5P). The final dataset of COI sequences included three new sequences of *A. clarkei*, one sequence of *A. xylogragma* and 13 sequences from other species of Acrolepiinae of the genera *Acrolepia, Acrolepiopsis* and *Digitivalva* from BOLD (Table 1). Two species of *Plutella* were used as the proximal outgroup as it is considered closely related to Glyphipterygidae (Mutanen et al., 2010).

Table 1
Specimens used to infer the phylogenetic status of *Antispastis clarkei* and relationship within the subfamily Acrolepiinae.

Family	Genus	Species	Voucher	BOLD COI-5P
Ingroup				
Glyphipterigidae				
	Antipastis	*clarkei*	LMCI 283-38A	MISA034-18
	Antipastis	*clarkei*	LMCI 283-38B	MISA035-18
	Antipastis	*clarkei*	LMCI 283-38C	MISA036-18
	Antipastis	*xylophragma*	KN-06-1146	LTOL977-08
	Digitivalva	*arnicella*	–	LEATC522-13
	Digitivalva	*granitella*	–	GMGMG1314-14
	Digitivalva	*reticulella*	–	FBLMV367-09
	Digitivalva	*pappella*	–	PHLSA372-11
	Digitivalva	*pulicariae*	–	CGUKC360-09
	Acrolepia	*autumnitella*	–	CGUKC918-09
	Acrolepiopsis	*assectella*	–	CGUKD144-09
	Acrolepiopsis	*californica*	–	MECD429-06
	Acrolepiopsis	*incertella*	–	LNEL257-06
	Acrolepiopsis	*heppneri*	–	LEFIJ1515-12
	Acrolepiopsis	*leucoscia*	–	LPOKE636-12
	Acrolepiopsis	*sapporensis*	–	LTOL943-08
	Acrolepiopsis	*vesperella*	–	PHLSA370-11
Outgroup				
Plutellidae				
	Plutella	*geniatella*	–	ABOLB348-15
	Plutella	*xylostella*	–	AGIMP029-14

Intra- and interspecific genetic distances were estimated using the Kimura 2-parameter model. Phylogenetic analysis was carried out using maximum likelihood (ML) implemented in PhyML 3.1 (Guindon et al., 2010). The best-fitting model was determined by jModelTest 2 (Darriba et al., 2012) based on the Akaike information criterion. Analysis for heuristic tree searches was performed using the GTR+I+G substitution model, TBR branch swapping and 100 bootstrap replications.

Morphological description

Specimens used in the illustrations presented in this study came from eggs and larvae collected on *Solanum johannae* Bitter (Solanaceae), from November 2014 to July 2018, in the Centro de Pesquisas e Conservação da Natureza (CPCN Pró-Mata/PUCRS; 29°28′36″S, 50°10′01″W), 900 m, São Francisco de Paula municipality, Rio Grande do Sul State (RS), Brazil. They were reared in small plastic vials under controlled conditions (14 h light/10 h dark; 25 ± 2 °C) in the Laboratório de Morfologia e Comportamento de Insetos, Departamento de Zoologia, Universidade Federal do Rio Grande do Sul (UFRGS), Porto Alegre city, RS. Adults were pin-mounted and dried. Immature stages were fixed in Dietrich's fluid and preserved in 75% ethanol. For descriptions of the adult morphology, the specimens were cleared in a 10% potassium hydroxide (KOH) solution, stained with either fuchsin acid or Chlorazol black E, and slide-mounted in Canada balsam. Wings were cleared with 5% sodium hypochlorite solution, stained with eosin, and mounted similarly on slides.

Observations were performed with the aid of a Leica® M125 stereomicroscope. Structures selected to be drawn were previously photographed with a Sony® Cyber-shot DSC-H10 digital camera mounted on the stereomicroscope. Vectorized line drawings were then made with the software Corel Photo-Paint® X7, using the corresponding digital photos as a guide. At least five specimens were used for the descriptions of each life stage or instar.

For scanning electron microscope analyses, specimens were dehydrated in a Bal-tec® CPD030 critical-point dryer, mounted with double-sided tape on metal stubs, coated with gold in a Baltec® SCD050 sputter coater, examined and photographed in a JEOL® JSM6060 scanning electron microscope at the Centro de Microscopia Eletrônica (CME) of UFRGS.

Histological preparations of larval mines were based on field-collected leaf samples (0.5 cm^2) containing mines ($n = 6$) fixed in 4% Karnovsky (2.5% glutaraldehyde and 4.5% formaldehyde in phosphate buffer 0.1 M, modified to pH 7.2) (O'Brien and McCully, 1981). The fixed fragments were dehydrated in an n-butyl series, embedded in Paraplast and sectioned transversely (12 μm) in a rotatory microtome (Jung Biocut). The sections were stained in safranin-astrablue (2:8, v/v) (Bukatsch, 1972, modified to 0.5%), mounted in colorless varnish (Paiva et al., 2006), and photographed under a Leica DM 2500-LED light microscope with a Leica DFC7000T camera.

Material examined

BRAZIL: Centro de Pesquisas e Conservação da Natureza Pró-Mata (CPCN Pró-Mata), 29°28′36″S, 50°10′01″W, São Francisco de Paula municipality, Rio Grande do Sul State (RS), either reared or dissected from mines associated with *Solanum johannae*: 04-07.XI.2014, G.R.P. Moreira, R. Brito & H. Vargas, legs., LMCI 306;

21-24.VI.2016, G.R.P. Moreira, R. Brito & J. Fochezato, legs., LMCI 306; 28-30.VI.2017, G.R.P. Moreira & J. Fochezato, legs., LMCI 319; 01-02.VII.2018, G.R.P. Moreira & J. Fochezato legs., LMCI 320. Luiz Laux farm, 29°37′59″S, 51°28′12″W, Montenegro municipality, RS, either reared or dissected from mines associated with *Solanum mauritianum*: 17.XI.2017, G.R.P. Moreira, R. Brito, C.M. Pereira, S. Steinstrasser & J. Fochezato legs., LMCI 322. Swampy area, Quatro Barras, Paraná State, reared from mines associated with *Solanum variabile*, 26.I.1970, Vitor O. Becker leg., VB 8876, donated to LMCI (313).

Immature stages, fixed in Dietrich and preserved in ethanol 70%: eggs (five – LMCI 320-15); first instar larvae (seven – LMCI 320-16); second instar larvae (nine – LMCI 320-68); third instar larvae (one – LMCI 320-17; six – LMCI 319-15); fourth instar larvae (eight – LMCI 320-18); pupae (four – LMCI 283-137); larvae preserved in ethanol 100%, under −20 °C for DNA extraction: five – LMCI 283-38; eight – LMCI 322-9; adults, with genitalia on slides: males (four – LMCI 283-119, 121; 313-858; 322-11, 12), females (five – LMCI 283-89, 90; 306-51, 313-856, 857).

Museum collections

Abbreviations of the institutions from which specimens were examined are:

LMCI: Laboratório de Morfologia e Comportamento de Insetos, Universidade Federal do Rio Grande do Sul, Porto Alegre, Rio Grande do Sul, Brazil.

VOB: Collection Vitor O. Becker, Reserva Serra Bonita, Camacan, Bahia, Brazil.

Results

Molecular analysis (Fig. 1)

A final dataset of 19 sequences with 658 nucleotides were analyzed, of which 245 sites (37%) were phylogenetically informative. The sequences of the three specimens of *A. clarkei* clustered, and the nearest neighbor was *A. xylophragma* (Fig. 1). This clade was recovered as sister to *Digitivalva*. Thus, together with *Acrolepiopsis*, *Acrolepia* and *Digitivalva*, the genus *Antispastis* is supported as part of Acrolepiinae, therefore placed within Glyphyperigidae (*sensu* Nieukerken et al., 2011). Pairwise genetic divergence of *A. clarkei* ranged from 10 to 15%, with lowest the distance to *A. xylophragma* and highest to *Acrolepia autumnitella* and *Plutella* spp. (Table 2).

Morphological description

Adults (Fig. 2)

They conform in color and general morphology to the original description and illustrations of *A. clarkei* provided by Pastrana (1951), including the diagnostic characters, the well-developed maxillary palpi (Fig. 2C) and fused A_{1+2} hindwing veins (Fig. 2B) that distinguish them from the most closely related species, *A. xylophragma*, according to this author. Small differences in the relative size of the male valva (Fig. 2E) and distance among clusters

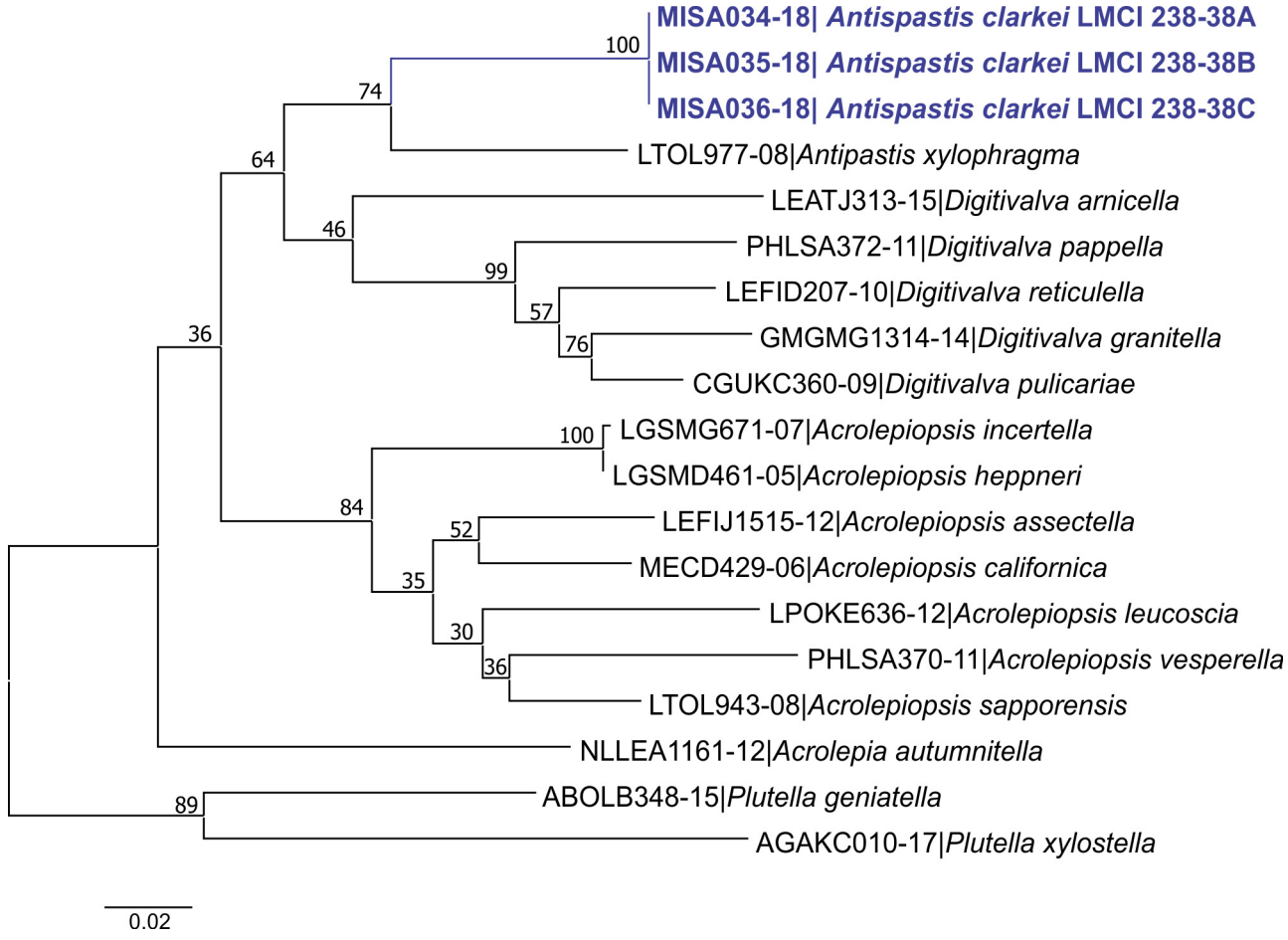

Fig. 1. Maximum likelihood consensus tree for *Antispastis* Meyrick inferred based on DNA barcode sequences (668 bp of the cytochrome oxidase subunit I gene). Numbers above branches indicate bootstrap support.

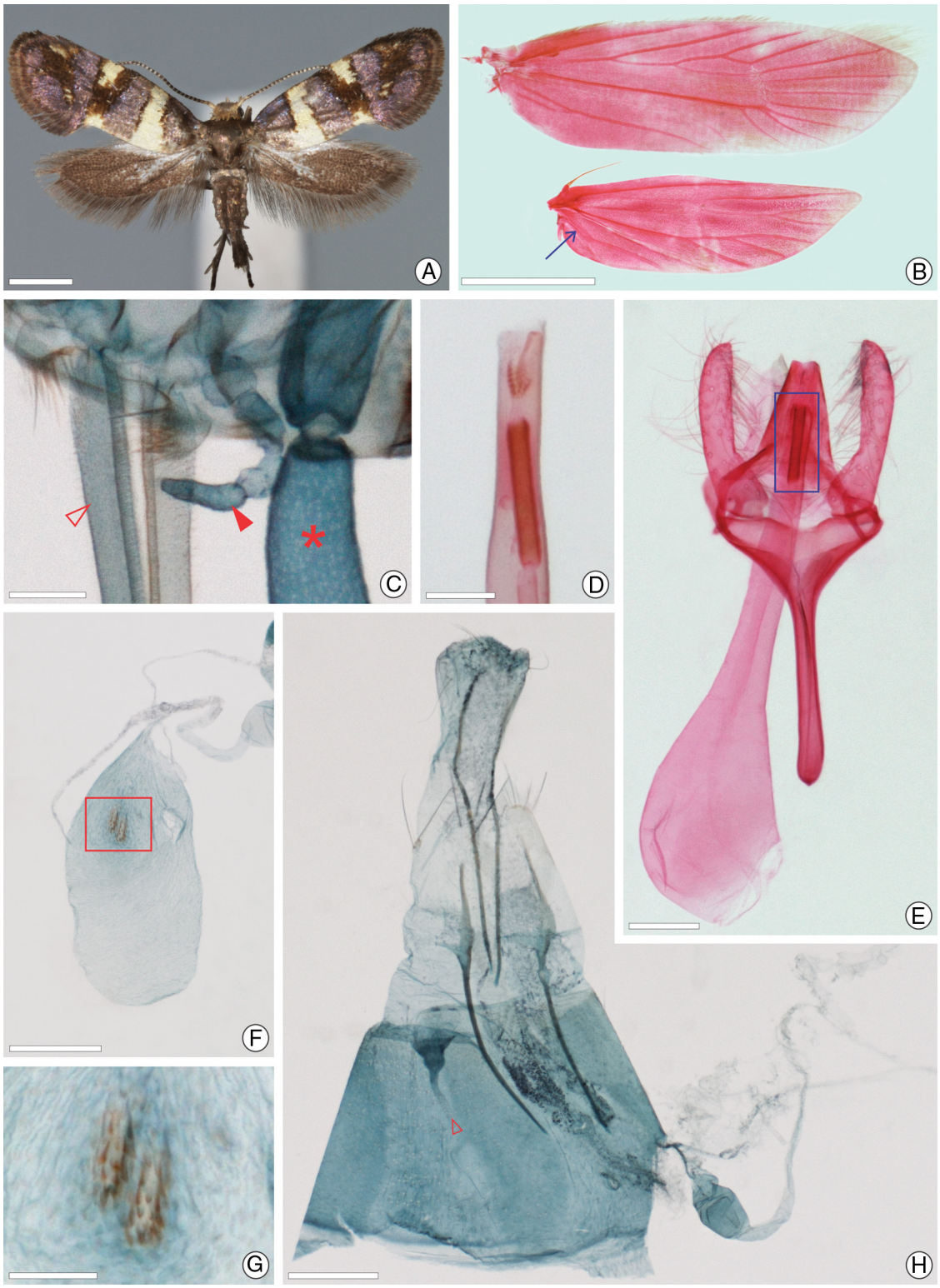

Fig. 2. Adult morphology of *Antispastis clarkei*: A, pinned-dried adult female, dorsal view; B, fore and hind wings, respectively, dorsal (seta points to fused A_{1+2} on hind wing); C, mouth parts, antero-dorsal (open and closed arrows indicate proboscis and maxillary palpus, respectively; asterisk marks labial palpus); D, vesica in detail, ventral (area marked with rectangle in E); E, male genitalia, ventral; F, corpus bursae, ventral; G, signum in detail (area marked with rectangle in F); H, female genitalia, ventral (open arrow points to missing distal portion of ductus bursae and corpus bursae, broken off during preparation). Scale bars = 1 mm (A, B); 50, 50, 100, 200, 100, 200 μm, from C to H, respectively.

of spines in the female signum (Fig. 2G) found among the Brazilian material studied here were considered variation at the population level, pending further comparison when specimens from additional localities are available.

Egg (Figs. 4A–C, 7A)

Dimensions; $n = 5$: Length = 0.44 ± 0.02 mm; width = 0.3 ± 0.01 mm. Flat and elliptical (Fig. 4A), deposited with the micropylar axis in parallel to the leaf; chorion

Table 2
Genetic distance between *Antispastis clarkei* and other members of Acrolepiinae based on 658 base pair sequences of the Cytochrome oxidase I (*COI*) gene using the Kimura 2-parameter model. Intra-group distances are shown in brackets.

		1.	2.	3.	4.	5.	6.
1.	*Antispastis clarkei*	[0.00]					
2.	*Antispastis xylophragma*	0.10	–				
3.	*Acrolepia autumnitella*	0.15	0.15	–			
4.	*Digitivalva* spp.	0.12	0.12	0.15	[0.10]		
5.	*Acrolepiopsis* spp.	0.14	0.13	0.13	0.13	[0.08]	
6.	*Plutella* spp.	0.15	0.16	0.17	0.17	0.16	[0.15]

Table 3
Variation in size among head capsules of *Antispastis clarkei* larvae reared on *Solanum johannae* Bitter.

Instar	*n*	Head capsule width (mm)		
		Mean ± standard error	Range	Growth rate
I	8	0.158 ± 0.004	0.137–0.169	–
II	9	0.226 ± 0.006	0.221–0.273	1.43
III	7	0.473 ± 0.007	0.420–0.494	2.09
IV	8	0.688 ± 0.010	0.630–0.704	1.46

translucent (Fig. 7A); surface smooth without defined carinae and cells (Fig. 4A). Micropylar area on anterior pole, with *ca.* ten sub-trapezoidal cells surrounding the micropyles (Fig. 4B). A few, scattered circular aeropyles with slightly elevated peritreme (Fig. 4C) on the latero-dorsal area.

Larva

Prognathous, with chewing-type mouthparts. Body creamy white (Fig. 7B) with light brown head capsule, and little-differentiated prothoracic dorsal shield and anal plate. There are four instars and two morphotypes; the first form corresponds to the first two, and the second to the last two instars. The first morphotype has a sub-cylindrical, mostly smooth body, with reduced thoracic legs and without specialized locomotor structures on the abdomen (Fig. 4D). The second morphotype has well-developed legs on the thorax and pseudopodia on the abdomen, and setae of variable sizes distributed throughout the body (Figs. 3A, 5). We could not find major morphological differences between instars within the first and second morphotypes. However, they can be identified by their size, since corresponding head capsule widths do not overlap (Table 3). The following exponential growth equation was adjusted for the head capsule width: $y = 0.092e^{0.506x}$; $n = 32$; $r = 0.98$; $p < 0.0001$.

First instar (Fig. 4D–N). Maximum length = 1.49 ± 0.02 mm; $n = 3$. Head depressed, subretangular, with lateral margin slightly convex (Fig. 4D, E); frontoclypeus subtriangular, well-marked by pigmented adfrontal sutures, extending to apex of epicranial notch; setation mostly reduced or absent. Labrum bilobed, sharply cleft at middle of distal margin; five pairs of highly modified, flatted setae on lateral margin, and one pair of filiform setae on center (Fig. 4G). Three ill-defined stemmata laterally (Fig. 4I). Antennae three-segmented (Fig. 4F, G); first and second segments wider than long; second segment with two stout sensilla on distal surface and four filiform sensilla laterally; third segment shorter and narrower, with one stout and two filiform sensilla distally. Mandible well developed with well-developed teeth, bearing two setae externally on proximal bases. Maxilla (Fig. 4G) with galea and palpus well developed, single seta and microsetae on galea and one filiform seta on palpus base. Labium (Fig. 4H) short, with a cylindrical spinneret apically; labial palpi laterally at bases of the spinneret, about half the length of spinneret and bi-segmented, each segment bearing a seta on distal margin. Chaetotaxy: All setae hair-like, reduced or absent; A group in bisetose, A1 similar in length to A3; S group in trisetose, S2 longer than S1 and S3, the latter reduced to a microseta; SS group unisetose. Thoracic legs reduced, with curved tarsal claws flanked on dorsum by large spatulate seta (Fig. 4J, K). Abdominal pseudopodia absent. Prothoracic spiracle cone-like, laterally, close to posterior margin of prothorax (Fig. 4L). Abdominal spiracles (Fig. 4M) with poorly-developed peritreme, laterally on A1–8, slightly displaced postero-dorsally. Thoracic and abdominal setae mostly absent or extremely reduced, except on last abdominal segment, where well developed, filiform setae are present (Fig. 4N). Chaetotaxy (A10): D and SD group in bisetose, SD2 longer than the other setae; L group with similar size, in trisetose; PP1 located posteriorly to L group; SV group composed by three setae close to each other; V group in unisetose.

Fourth instar (Figs. 3A, 5, 7B). Maximum length = 5.01 ± 0.40 mm; $n = 4$. Head depressed, subretangular, with lateral margin slightly convex (Fig. 5A–C); frontoclypeus subtriangular, well-marked by pigmented adfrontal sutures, extending to apex of epicranial notch. Labrum bilobed, sharply cleft at middle of distal margin; five pairs of highly modified, flattened setae on lateral margin and one pair of filiform setae on center (Fig. 5E). Five stemmata well delimited laterally; stemma 2 reduced (Fig. 5D). Antennae three-segmented (Fig. 5F); first segment shorter than second, bearing two small sensilla on distal margin; second segment with two stout sensilla and three filiform setae on distal margin; third segment narrower and shorter, with one stout and two filiform sensilla distally; antocoria covered with rounded tubercules, strongly developed, projecting meso-anteriorly to mandible base. Mandible well developed with well-developed teeth, bearing two setae externally on proximal base. Maxilla (Fig. 5C) with galea and palpus well developed and four filiform setae, two on galea and one on first and on second palpomere. Labium (Fig. 5G) short with two filiform setae on base and a cylindrical spinneret apically; labial palpi with two basal setae, palpi laterally at basis of the spinneret, about half-length of spinneret and bi-segmented, each segment bearing a seta on distal margin; distal segment shorter and narrower. Chaetotaxy: All setae hair-like. A group bisetose, A1 similar in length to A3; S group trisetose, S2 longer than S1 and S3; SS group bisetose, SS1 more ventral, closest to mandibles; AF unisetose, AF2 closest to ecdysial line; L group unisetose, L1 posterior to A3; P2 greatly reduced, located posteriorly between L1 and AF2; CD group trisetose, all reduced to microsetae; MG group bisetose, all short. Thorax (T) and abdomen (A) mostly covered by dense filiform microtrichia (Fig. 5H, I, M–O). Thoracic legs well developed, with curved tarsal claws flanked laterally by a pair of large spatulate seta (Fig. 5K, L); filiform setae, five on coxa and two on femur, tibia and tarsus. Prothoracic dorsal shield (Fig. 5H) and anal plate (Fig. 5O) rounded and smooth, covering most of T1 and A10 dorsally. Additional rounded, smooth plates, ventrally on T1 and latero-dorsally on A8 and A9. Spiracles cone-like (Fig. 5J), with small, circular aperture on apex; located latero-dorsally, close to posterior margin on T1, slightly displaced antero-dorsally on A1-7 and postero-ventrally on A8. Abdominal pseudopodia on A3–6, and A10; crochets uniordinal in uniserial circles on A3–A6, half circle on A10. Chaetotaxy: All setae hair-like, length variable. Prothorax: XD bisetose, with similar length, close to margin anterior of shield dorsal; D group bisetose, in dorsal shield, D1 slightly smaller than D2; SD group bisetose, on lateral margin of dorsal shield, SD1 anterior and larger than SD2, the latter with similar length to D2; L group bisetose, anterior to spiracle which is close to posterior margin of segment, L2 longer than L1; SV group bisetose on smooth plate latero-dorsal to the coxa; V1 on the underside of the coxa. Meso-metathorax: MD unisetose and MSD bisetose, all greatly reduced, MD1 dorsal to MSD1 and MSD2; D group bisetose, D1 anterior to D2; SD group bisetose, SD2 antero-dorsally to and slightly smaller than SD1; L group trisetose, with similar length; V group unisetose, close to coxa. Abdomen: A1–2: MD group unisetose, similar to meso and metathorax; D group bisetose, D1 antero-ventrally and smaller than D2; SD group bisetose,

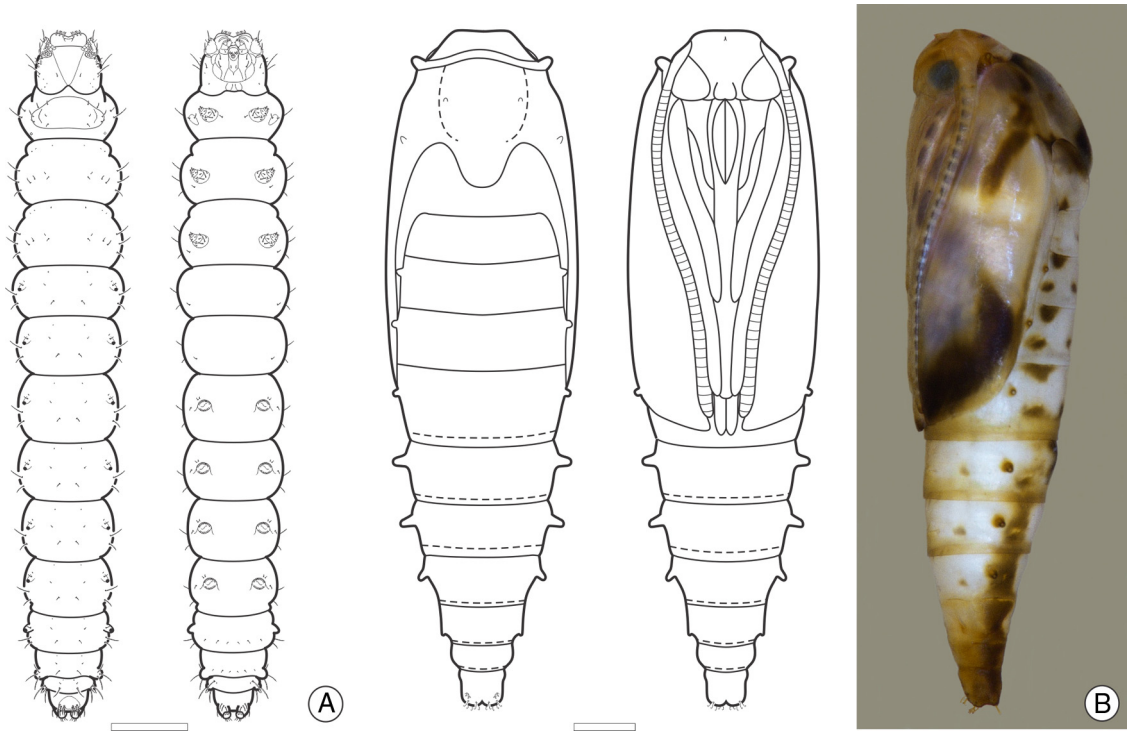

Fig. 3. Larval and pupal morphology of *Antispastis clarkei* under light microscopy: A, last larval instar, under dorsal and ventral views; B, pupa, dorsal, ventral and lateral, respectively. Scale bars = 0.5 mm.

SD2 larger than SD1, the last antero-dorsal to SD2; L group bisetose, postero-ventral to spiracle, L2 larger than L1; V group unisetose. A3–6: similar to preceding segment, but SV group bisetose closest to pseudopodia. A7: similar to A1–2, but SD group unisetose on spiracle and six setae equidistant on ventral region (=SV bisetose + V group unisetose). A8: similar to A7, but SD group absent and L group trisetose on smooth plate lateral. A9: MD group and D group similar to A8, but D2 much longer than D1; L group trisetose, on lateral plate; SV group bisetose, SV1 longer and SV2 greatly reduced. A10: D and SD groups on anal shield, bisetose; L group trisetose close to PP1; SV group tetrasetose, closest to pseudopodia and V group unisetose, with similar length to SV group setae.

Pupa (Figs. 3B, 6)

Maximum length of specimens examined ranged from 4.01 to 5.23 mm ($n = 4$). General coloration whitish-light brown, with head, thorax and corresponding appendices darkening later in development, and abdomen with dark-brown blotches on central dorsum and laterally. Body surface rough, sparsely covered with small, irregular shaped tubercles. Vertex bearing small, subtriangular acute process (=cocoon cutter; Fig. 6B, C). Frons without frontal setae (Fig. 6B). Antennae and forewing extending to posterior margin of fourth abdominal (A4) segment; proboscis reaching middle of A4; prothoracic, mesothoracic and metathoracic legs extending to A2, middle of A4 and posterior margin of A4, respectively (Fig. 3B). Acute tubercles on middle-posterior section of each forewing base (Fig. 6A). Spiracles conical-shaped, with peritreme strongly elevated; prothoracic ones (Fig. 6F) stouter; the aperture is a slit located on the latero-posterior margin; from A2 to A7 they vary in length and have distally located, circular apertures (Fig. 6G). Spiracles are not visible externally on A1, partially closed on A8 (Fig. 6H). A pair of short setae on posterior section of mesothoracic terga (Fig. 6E). A pair of similar setae adjacent to spiracles from A2 to A8 (Figs 6G, H), and two pairs latero-dorsally on distal margin of last segment (Fig. 6I, L). Last abdominal segment forming two short, dorsal distal lobes, and bearing *ca.*14 stout, distally curved hooks, mostly distributed ventrally, forming a cremaster (Fig. 6I–K).

Natural history

The translucent eggs of *A. clarkei* are laid on the abaxial leaf surface, attached with an unidentified adhesive substance, close to the midrib or secondary veins (Fig. 7A). After hatching, the first instar larva penetrates the abaxial epidermis, where it starts the mine by cutting the anticlinal cell walls of the first tissue layer adjacent to the adaxial epidermis (Fig. 8A, B). The mine is constructed exclusively within palisade parenchyma cells, whose cell wall fragments remain lining the mine (Fig. 8C–E). Initially the mine is more or less linear and narrow (Fig. 7E), increasing in width slightly during the first two instars. After molting to the third instar the mine turns into a blotch type, which at first usually shows finger-like projections, and later in development may cover most of the lamina on small leaves (Fig. 7D, E, H). As already described by Bourquin (1951), the blotch section of these mines is deprived of feces, which are discharged through a semicircular orifice made on the abaxial epidermis by positioning the distal portion of the abdomen outside the mine (Fig. 7C). Feces are laid around the discharge orifice, frequently embedded in a dark brown, liquid substance (Fig. 7F). Before pupation, the last larval instar leaves the mine, constructing an inverted basket-like, wide-meshed, brown cocoon (Fig. 7I), usually on the plant surface. At emergence, the adult leaves the cocoon through a dorsal slit located on the distal margin (Fig. 7G) toward which the pupal head is positioned. Pupal exuvia remain inside the cocoon after emergence.

At the CPCN Pró-Mata, São Francisco de Paula municipality, *A. clarkei* mines were relatively common on *S. johannae* plants, particularly on young plants located under shaded, humid areas of road borders, where many leaves may be mined per plant (Fig. 7D). Our

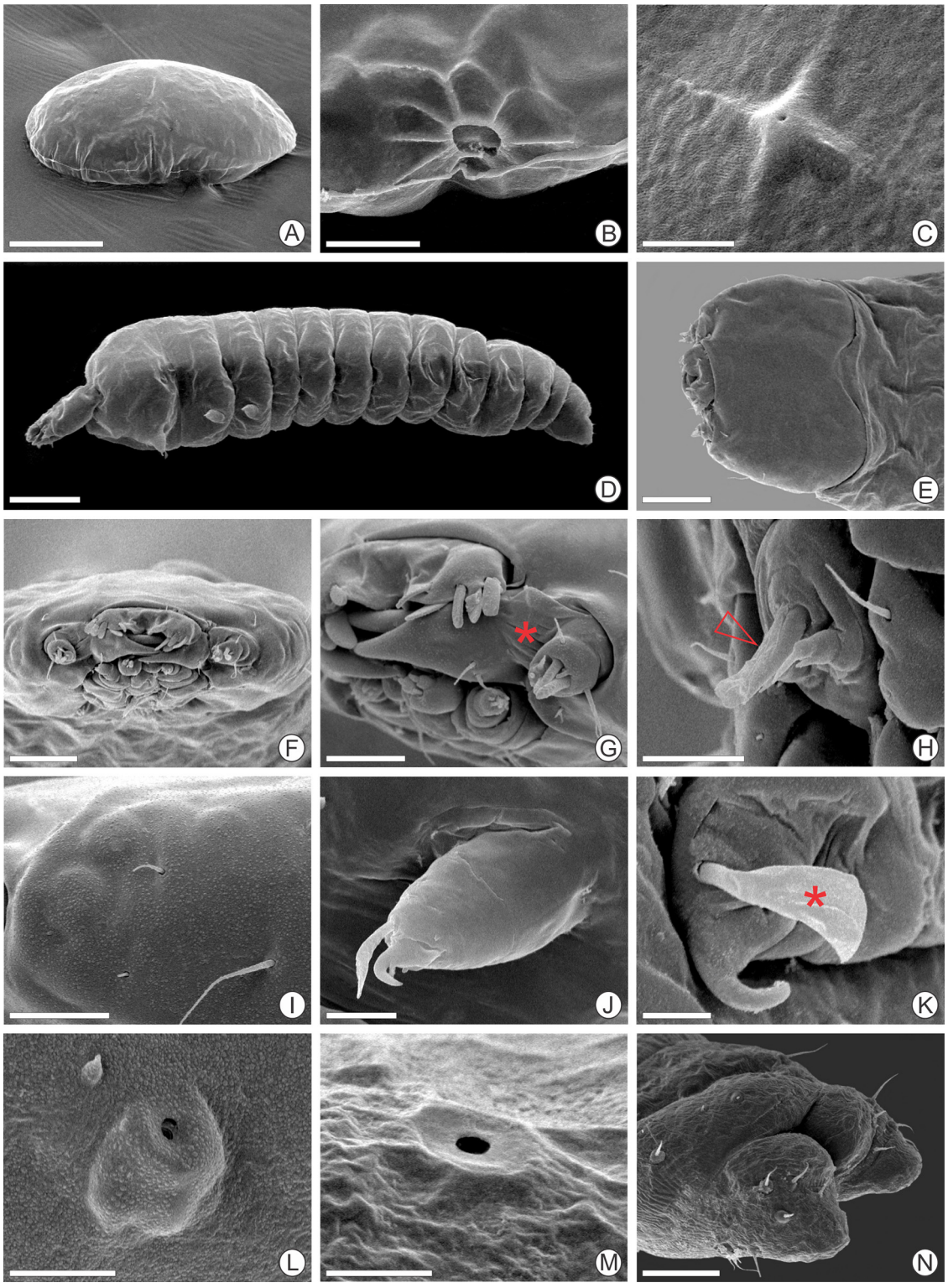

Fig. 4. Scanning electron micrographs of *Antispastis clarkei* egg (A–C) and first larval instar (D–N): A, general view of egg, latero-dorsal; B, micropylar region on anterior pole, lateral; C, aeropyle, dorsal; D, general view of first instar, lateral; E, F, head, dorsal and anterior, respectively; G, detail of mandible, antenna and maxilla, antero-lateral (asterisk indicates corrugated nature of the mandibular base in association with the antennal antocoria); H, labium, antero-lateral (arrow indicates spinneret); I, stemmata, lateral; J, mesothoracic leg, postero-dorsal; K, tarsal claw in detail, mesal (asterisk indicates associated spatulate seta); L, M, prothoracic and third abdominal spiracles lateral; N, last abdominal segments postero-dorsal. Scale bars = 150, 15, 5, 100, 50, 30, 15, 10, 10, 10, 5, 10, 5, 20 μm, respectively.

field collection data suggested this species has at least two generations per year in Rio Grande do Sul state, the lowest densities of immature stages appearing during late summer and autumn (from March to June).

Discussion

Adults of *A. clarkei* examined in the present study conform in external morphology to Acrolepiinae (Glyphipterigidae, Yponomeutoidea; *sensu* Nieukerken et al., 2011), particularly in

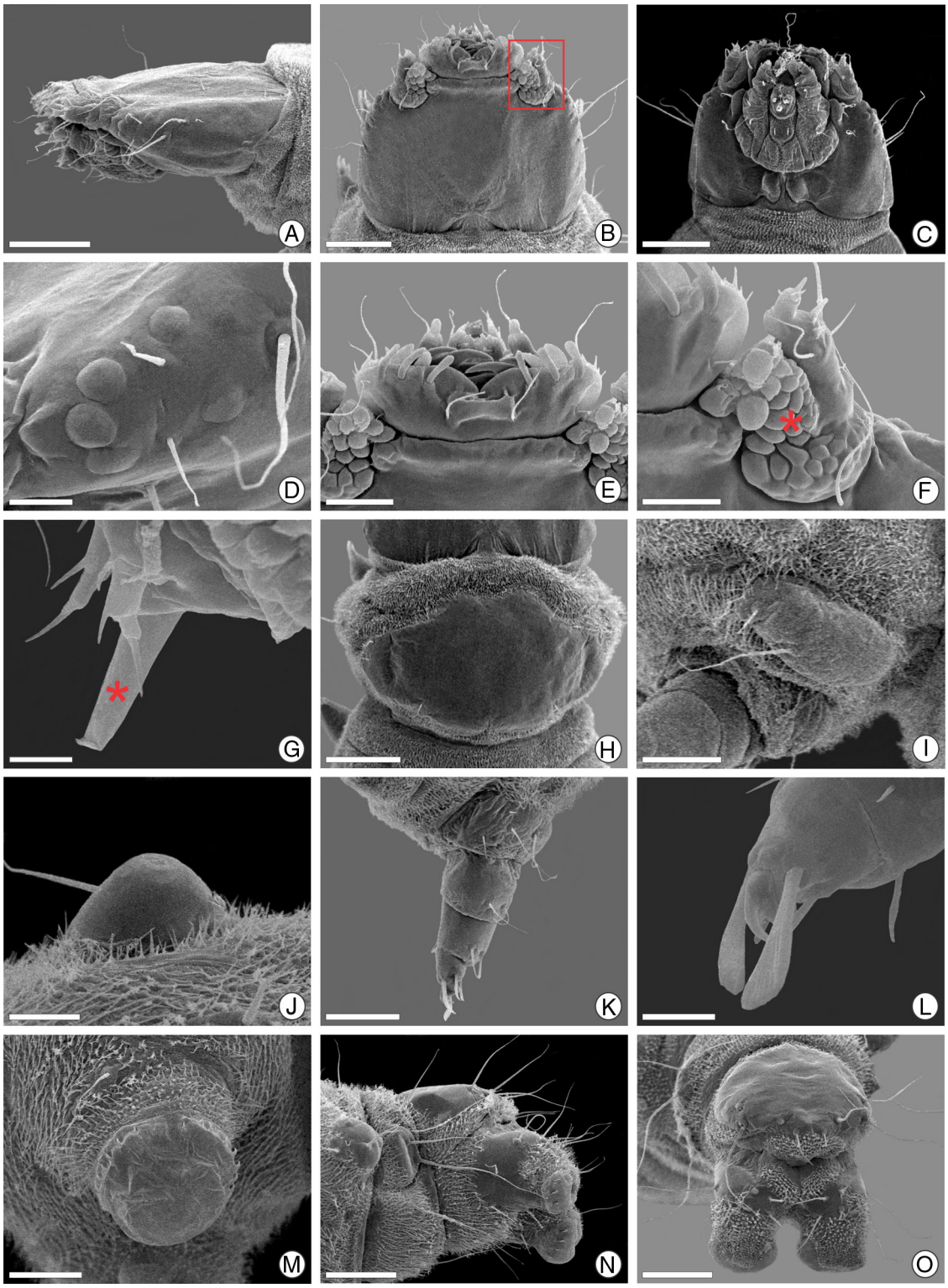

Fig. 5. Scanning electron micrographs of *Antispastis clarkei* fourth (last) larval instar: A–C, head, under lateral, dorsal and ventral views, respectively; D, stemmata, lateral; E, labrum, dorsal; F, antenna, dorsal (asterisk indicates expanded antocoria); G, labium, lateral (asterisk indicates the spinneret); H, prothoracic dorsal shield, dorsal; I, prothoracic upper-coxal plate, lateral; J, spiracle of second abdominal segment, latero-ventral; K, mesothoracic leg, mesal; L, pretarsus in detail, latero-posterior; M, pseudopodium of third abdominal segment, latero-ventral; N, O, last abdominal segments, lateral and posterior, respectively. Scale bars = 200, 150, 200, 30, 50, 40, 10, 200, 80, 40, 100, 20, 80, 150, 150 μm, respectively.

relation to the mouthparts, wing venation and genitalia (for a detailed description see Landry, 2007, as Acrolepiidae), a taxonomic position supported also by the molecular analyses. In the phylogeny inferred here, it was closest to the genus *Digitivalva.* Their DNA sequences presented approximately 10% genetic divergence in relation to a specimen of *A. xylophragma* from BOLD. Such high divergence between species of the same genus has been found in other genera of Glyphipterigidae (e.g. *Acrolepiopsis*) and Plutellidae (Landry, 2007). We also observed high divergence within Acrolepiinae genera (12% in *Digitivalva*). This highlights the

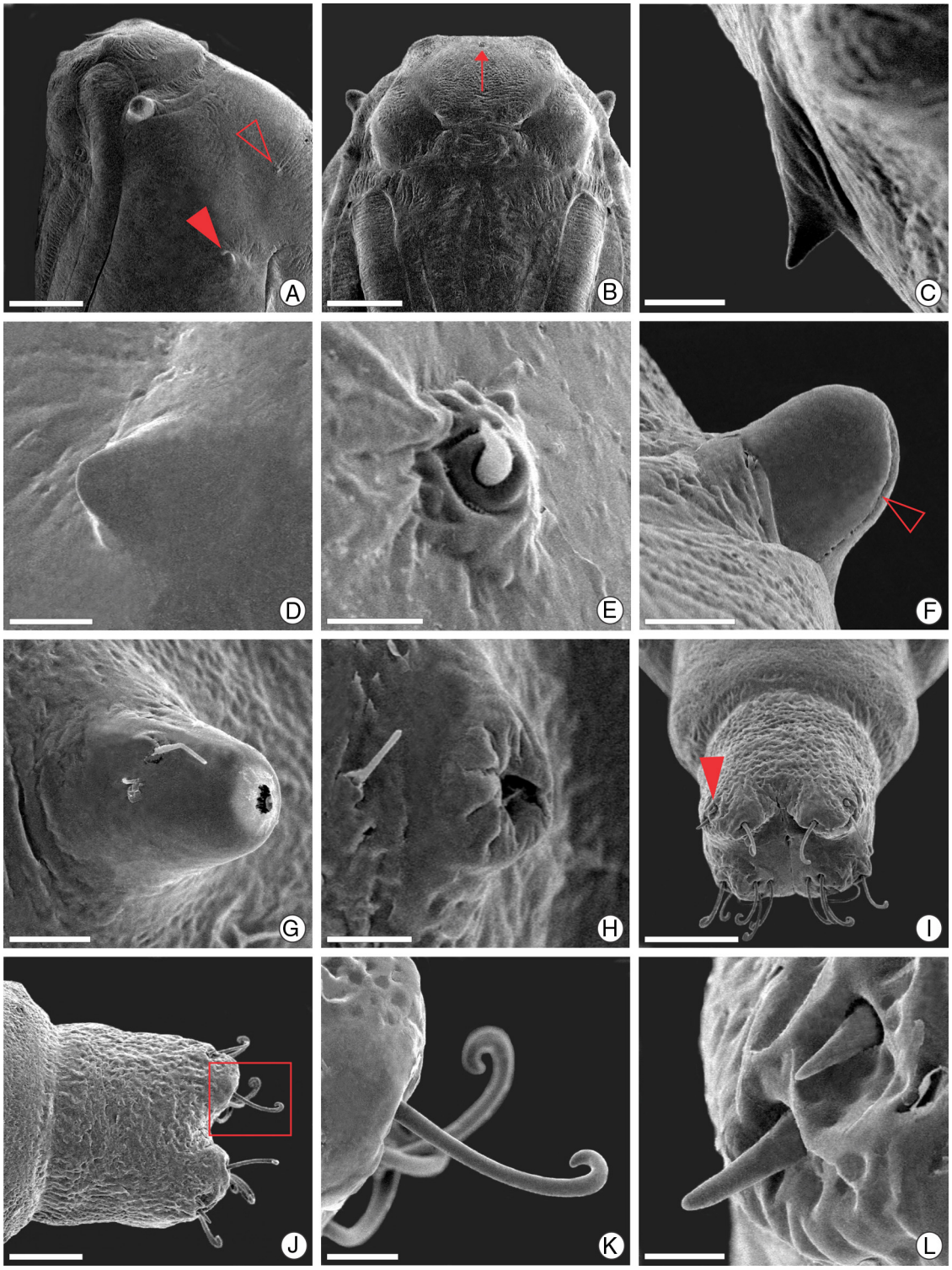

Fig. 6. Scanning electron micrographs of *Antispastis clarkei* pupa: A, B, head and anterior portion of thorax, lateral and ventral views, respectively; C, cocoon cutter, lateral (indicated by seta in B); D, basal tubercle of forewing, lateral (indicated by closed arrowhead in A); E, latero-dorsal micro-seta of mesothorax, lateral (indicated by open arrowhead in A); F, prothoracic spiracle, dorsal (open arrowhead indicates latero-posterior slit); G, H, spiracles of seventh and eighth abdominal segments, respectively, lateral; I, J, last abdominal segments, dorso-posterior and dorsal, respectively; K, cremaster hooks in detail (enlarged area marked with a rectangle in J); L, latero-dorsal setae of last abdominal segment, posterior (area indicated by closed arrow in I). Scale bars = 250, 200, 30, 30, 20, 30, 30, 20, 150, 100, 20, 10 μm, respectively.

genetic and morphological diversity of lineages within Glyphypterigidae, which suggests a need for taxonomic revision. It might also indicate an ancient diversification process that has fixed several differences. Although COI has been useful as a first phylogenetic approach, more genes are necessary to make robust and broader inferences, and thus to make decisions regarding status at and above the genus level in this complex group of glyphipterigids.

The elevated spiracles described here give further support that the genus *Antispastis* belongs to Yponomeutoidea, in addition to presence of abdominal pleural lobes in the adult, a defining

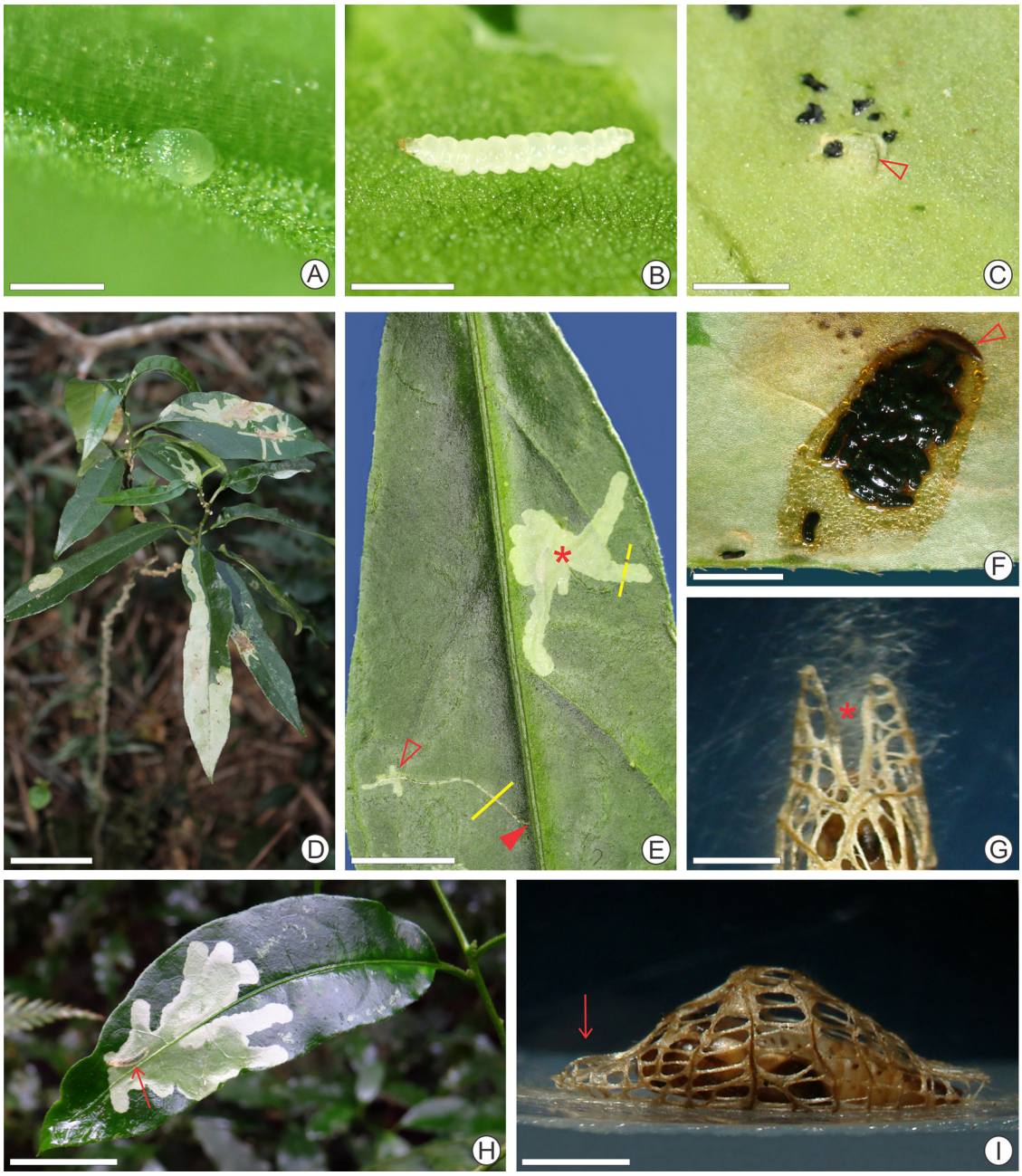

Fig. 7. Natural history of *Antispastis clarkei* on *Solanum johannae*: A, egg on abaxial surface of *S. johannae* leaf; B, last larval instar within dissected mine; C, a discharge orifice of a young blotch mine (aperture indicated by arrow) on leaf abaxial surface, surrounded by isolated small fecal pellets; D, young host plant showing leaf mines of varied ages and shapes on adaxial surface of leaves; E, young leaf mines in detail; beginning and end of a first-instar, filiform mine are indicated by closed and open arrows, respectively; asterisk indicates a third instar, blotch mine; dashed and broken lines mark location of histological sections presented in Fig. 8; F, feces embedded in brownish liquid, discharged by a full-grown larva (aperture of orifice also indicated by arrow); G, anterior aperture (asterisk) of cocoon in detail, dorsal; H, a last instar larva seen by transparency (arrow) within a large blotch mine; I, cocoon, general view, with pupa inside, constructed on the wall of a rearing plastic vial in laboratory, lateral. Scale bars = 0.3, 1.5, 20, 40, 15, 20, 0.5, 20, 1 mm, respectively.

synapomorphy for the superfamily. This kind of spiracle has been found in the larvae of Glyphipterigidae (*sensu* Nieukerken et al., 2011), appearing also in the pupal abdomen of members belonging to the three corresponding subfamilies (see Patočka and Turčani, 2005). Pupal thoracic spiracles born on a prominent process as described here have been apparently found only in the Glyphipteriginae (see Dugdale et al., 1998, as Glyphipterigidae). Lacelike, large-meshed cocoons as described for *A. clarkei* have been reported for other members of the Glyphipterigidae. But they are not unique to this family, being reported for other yponomeutoids such as Yponomeutidae and Plutellidae (Heppner, 1987) and even other lower Ditrysia such as Urodidae (Heppner, 1997; Adamski et al., 2009). Thus immature stages of *Antispastis* apparently share characteristics with more than one yponomeutoid family, and these aspects should be taken into account in corresponding phylogenetic studies in the future.

Larvae of glyphipterigids are supposed to have only six setae on the ninth abdominal segment (Heppner, 1987; Landry, 2007), which is not the case for *A. clarkei*, which has eight (five long and three short), which thus makes it similar to plutellids in this regard. Chaetotaxy of *A. clarkei* may differ from glyphipterigids and plutellids in which subdorsal setae are unisetose in A1–8 (see Heppner,

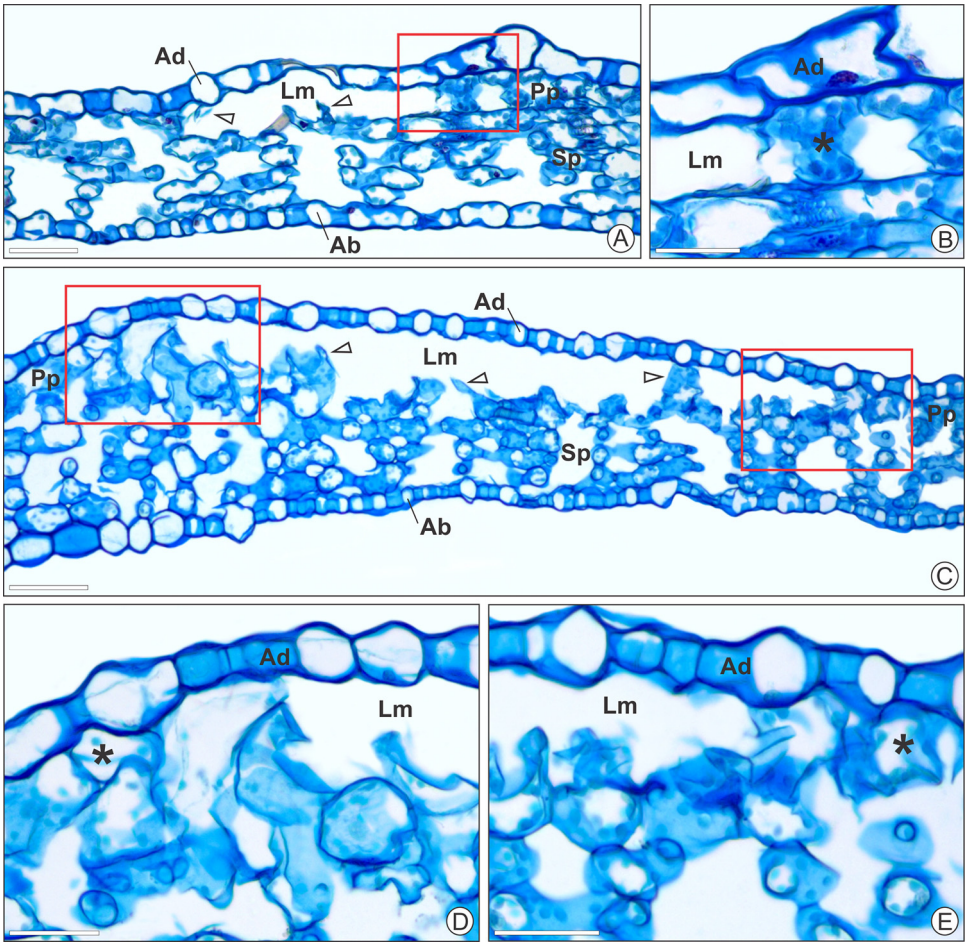

Fig. 8. Transverse histological sections of *Antispastis clarkei* mine on *Solanum johannae* leaves. A, initial, filiform portion (location indicated by unbroken line in Fig. 7E); B, detail of initial portion (enlarged area marked with a rectangle in A) with cut anticlinal cell wall of palisade parenchyma cells; C, final, blotch portion (location indicated by dashed line in Fig. 7E); D, E, details of blotch portion (enlarged areas marked with rectangles in C) with intact cells in adaxial epidermis and spongy parenchyma. Asterisks indicate intact cells of palisade parenchyma. Open arrows indicate cellular fragments left on palisade parenchyma after insect feeding. Ab, abaxial epidermis; Ad, adaxial epidermis; Lm, leaf mine; Pp, palisade parenchyma; Sp, spongy parenchyma. Scale bars = 50, 40, 100, 50, 50 μm, respectively.

1987), by having two such setae on A1–A6. We could not find any record for other Lepidoptera regarding the conspicuous antocoria present on *A. clarkei*, which should be further studied. This structure may extend internally into the mandibular base. It should be explored from a functional perspective, which is beyond the scope of the present study. The antocoria is not a segment, but the antennal socket (Hasenfuss and Kristensen, 1998) found in lepidopterous larvae. It remains uncertain whether this variation in morphology may be unique to *Antispastis*. It is atypical, since modifications of antennae of endophytic larvae of lepidopterous are usually associated not with expansion, but with reduction and loss of segments (Scoble, 1992).

Olckers et al. (2002) recorded *A. xylophragma* as a leaf miner of *S. mauritianum* (Alvear and Ituzaingo/Corrientes; Colonia Benitez/Chaco) and *S. fastigiatum* Willd. (Santo Tomé/Corrientes) in Argentina. Pedrosa-Macedo et al. (2003) also found this species as leaf miner of *S. mauritianum* in Brazil (Paraná state). Santos et al. (2008, 2009) reported the immature stages of *A. xylophragma*, with similar phenology to that found here, for the same population we studied at Montenegro. In that study they were associated with mines in *Solanum* L. species, including *S. mauritianum* and *Nicotiana alata* Link & Otto, and other non-Solanaceae, herbaceous plants (*Baccharis anomala* DC, Asteraceae; *Ipomoea cairica* (L.) Sweet, Convolvulaceae). As already mentioned, we could not find major morphological differences between specimens reared from *S. mauritianum* at the same locality compared to those attributed to *A. clarkei*. Data on *A. xylophragma* are scarce, being available only for the Peruvian type (morphology of male; female is unknown) and one specimen from Costa Rica (DNA sequence used in the present study). Apparently, these species cannot be distinguished by differences in color, thus the identification of *A. xylophragma* specimens surveyed by these authors should be further examined. A taxonomic review of the genus is clearly needed, pending on description of the immature stages and females of *A. xylophragma* and *A. selectella*.

Field collections indicate that the *A. clarkei* is oligophagous, using preferentially species of *Solanum* as hosts, which may vary within and among localities. At São Francisco de Paula municipality it has also been occasionally collected in association with *Solanum flaccidum* Vell. Our data expand the geographic distribution of *A. clarkei* from Argentina (Buenos Aires) to the Southern Atlantic Forest (Rio Grande do Sul and Paraná states, Brazil). Apparently, *Antispastis* specimens are rare in insect collections; as other acrolepiids, they may not be much attracted to light, and to light traps as a consequence (Landry, 2007). Thus it is likely that the geographical distribution of *A. clarkei* is broader, and that other congeneric species may be discovered when searching for and rearing their immatures are performed in the future throughout the Neotropical region.

Conflicts of interest

The authors declare no conflicts of interest.

Acknowledgements

Thanks are due to the Instituto de Meio Ambiente/PUC-RS (PROMATA, São Francisco de Paula) for allowing us to collect the specimens in areas under their care, and for providing assistance with fieldwork. We acknowledge the staff members of CME/UFRGS and Thales O. Freitas (UFRGS) for the use of facilities and assistance with scanning electron microscopy and molecular analyses, respectively. We are especially grateful to Vitor O. Becker (Reserva Serra Bonita) for supplying specimens from his collection and for providing information on *A. clarkei* paratypes. We thank Jeremy Dewaard (University of Guelph) and Peter Huemer (Tiroler-Landesmuseen) for making available sequence of *A. xylophragma*. Sérgio L. Bordignon (Universidade LaSalle) identified the plants. Thanks are also due to Lafayette Eaton for editing the text. We are especially grateful to Jean-François Landry (Agriculture and Agri-Food Canada) and one anonymous reviewer whose suggestions improved substantially the last version of the manuscript. G.R.P. Moreira, R.M.S. Isaias, R. Brito, J. S. Silveira Jr., and G.L. Gonçalves were supported by fellowships from CNPq, PDJ/CNPq, PROPESQ/UFRGS and CAPES, respectively.

References

Adamski, D., Boege, K., Landry, J.F., Sohn, J.C., 2009. Two new species of *Wockia* Heinemann (Lepidoptera: Urodidae) from coastal dry-forests in western México. Proc. Entomol. Soc. Washington 111, 166–182.

Bourquin, F., 1951. Notas sobre la metamorfosis de "*Antispastis clarkei*" Pastrana, 1951 (Lep "Glyphipterygidae"). Acta Zool. Lilloana 12, 523–526.

Bukatsch, F., 1972. Bermerkungen zur Doppelfärbung Astrablau-Safranin. Mikrokosmos 61, 255.

Clarke, J.F.G., 1969. Catalogue of the type specimens of Microlepidoptera in the British Museum (Natural History) described by Edward Meyrick. Glyphipterygidae, Gelechiidae (A-C) 6, 1–537 [Trustees of the British Museum, London].

Darriba, D., Taboada, G.L., Doallo, R., Posada, D., 2012. jModelTest 2: more models, new heuristics and parallel computing. Nature Methods 9, 772.

Davis, D.R., 1980. A redescription of "*Micropteryx*" *selectella* Walker with a discussion concerning its family affinities (Acrolepiidae). J. Lepid. Soc. 34, 187–190.

Dugdale, J.S., Kristensen, N.P., Robinson, G.S., Scoble, M.J., 1998. The Yponomeutoidea. In: Lepidoptera, Moths and Butterflies. Vol. 1: Evolution, Systematics, and Biogeography. Handbook of Zoology, Arthropoda: Insecta, Part 35. Walter de Gruyter, Hawthorne, pp. 119–130.

Folmer, O., Black, M., Hoeh, W., Lutz, R., Vrijenhoek, R., 1994. DNA primers for amplification of mitochondrial cytochrome c oxidase subunit I from diverse metazoan invertebrates. Mol. Mar. Biol. Biotechnol. 3, 294–299.

Gaedike, R., 1997. Acrolepiidae. In: Lepidopterorum Catalogus (New Series), Fasc. 55. Association for Tropical Lepidoptera and Scientific Publishers, Gainesville, pp. 1–16.

Guindon, S., Dufayard, J.F., Lefort, V., Anisimova, M., Hordijk, W., Gascuel, O., 2010. New algorithms and methods to estimate maximum-likelihood phylogenies: assessing the performance of PhyML 3.0. Syst. Biol. 59, 307–321.

Hasenfuss, I., Kristensen, 1998. Skeleton and muscles: immatures. In: Lepidoptera, Moths and Butterflies. Vol. 2: Evolution, Systematics, and Biogeography. Handbook of Zoology, Arthropoda: Insecta, Part 36. Walter de Gruyter, Hawthorne, pp. 133–164.

Heppner, J.B., 1984. Acrolepiidae. In: Heppner, J.B. (Ed.), Atlas of Neotropical Lepidoptera. Checklist: Part 1. Micropterigoidea-Immoidea. W. Junk, The Hague, p. 57.

Heppner, J.B., 1987. Acrolepiidae (Yponomeutoidea). In: Stehr, F.W. (Ed.), Immature Insects, vol. 1. Kendall-Hunt, Dubuque, pp. 409–410.

Heppner, J.B., 1997. *Wockia asperipunctella* in North America (Lepidoptera: Urodidae: Galacticinae). Holarct. Lepid. 4, 73–74.

Kyrby, J., 1984. The Yponomeutoidea: a reassessment of the superfamily and its suprageneric groups (Lepidoptera). Entomol. Scand. 15, 71–84.

Landry, J.-F., 2007. Taxonomic review of the leek moth genus *Acrolepiopsis* (Lepidoptera: Acrolepiidae) in North America. Can. Entomol. 139, 319–353.

Meyrick, E., 1912. Adelidae, Micropterygidae [sic], Gracilariadae [sic]. In: Wagner, H. (Ed.), Lepidopterorum Catalogus. Par. 6. W. Junk, Berlin, pp. 1–68.

Meyrick, E., 1926. Exotic Microlepidoptera 3, 307.

Mutanen, M., Wahlberg, N., Kaila, L., 2010. Comprehensive gene and taxon coverage elucidates radiation patterns in moths and butterflies. Proc. R. Soc. B 277, 2839–2848.

Nieukerken, E.J.V., Kaila, L., Kitching, I.J., Kristensen, N.P., Lees, D.C., et al., 2011. Order Lepidoptera Linnaeus, 1758. In: Animal biodiversity: An outline of higher-level classification and survey of taxonomic richness (ed. Zhang Z-Q). Zootaxa 3148, 212–221.

O'Brien, T.P., McCully, M.E., 1981. The Study of Plant Structure Principles and Selected Methods. Termarcarphi, Melbourne, pp. 345.

Olckers, T., Medal, J.C., Gandolfo, D.E., 2002. Insect herbivores associated with species of *Solanum* (Solanaceae) in Northeastern Argentina and Southeastern Paraguay, with reference to biological control of weeds in South Africa and the United States of America. Florida Entomol. 85, 254–260.

Paiva, J.G.A., Fank-De-Carvalho, S.M., Magalhães, M.P., Graciano-Ribeiro, D., 2006. Verniz vitral incolor 500®: uma alternativa de meio de montagem economicamente viável. Acta Bot. Brasil. 20, 257–264.

Pastrana, J., 1951. Una especie nueva de "Glyphipterygidae" de la Argentina (Lepidoptera). Acta Zool. Lilloana 12, 519–522.

Patočka, J., Turčani, M., 2005. Lepidoptera Pupae. Central European Species. Apollo Books, Stenstrup, pp. 542.

Pedrosa-Macedo, J.H., Olckers, T., Vitorino, M.D., Caxambu, M.G., 2003. Phytophagous arthropods associated with *Solanum mauritianum* Scopoli (Solanaceae) in the First Plateau of Paraná Brazil. A cooperative project on biological control of weeds between Brazil and South Africa. Neotrop. Entomol. 32, 519–522.

Ratnasingham, S., Hebert, P.D.N., 2007. BOLD: The Barcode of Life Data System (http://www.barcodinglife.org). Mol. Ecol. Notes 7, 355–364.

Santos, J.P., Redaelli, L.R., Dal Soglio, F.K., 2008. Plantas hospedeiras de lepidópteros ninadores em pomar de citros em Montenegro-RS. Rev. Brasil. Fruticult. 30, 255–258.

Santos, J.P., Redaelli, L.R., Dal Soglio, F.K., Foelke, E., Costa, V.A., 2009. Variação sazonal de lepidópteros minadores e seus parasitoides em plantas de crescimento espontâneo em pomar orgânico de citros em Montenegro, RS Brasil. Arq. Inst. Biol. 76, 381–391.

Scoble, M.J., 1992. The Lepidoptera: Form Function and Diversity. Oxford University Press, Oxford, pp. 404.

Sohn, J.-C., Regier, J.C., Mitter, C., Davis, D., Landry, J.-F., Zwick, A., Cummings, M.P., 2013. A molecular phylogeny for Yponomeutoidea (Insecta, Lepidoptera Ditrysia) and its implications for classification, biogeography and the evolution of host plant use. PLoS ONE 8 (1), e55066.

Walker, F., 1863. List of the specimens of lepidopterous insects in the collection of the British Museum. Vol. 28. Tortricites and Tineites. British Museum (Nat. Hist.), London, pp. 561.